

Incoherent charge dynamics of $\text{La}_{2-x}\text{Sr}_x\text{CuO}_4$: Dynamical localization and resistivity saturation

K. Takenaka,* J. Nohara, R. Shiozaki, and S. Sugai

Department of Physics, Nagoya University, Nagoya 464-8602, Japan

(Received 9 July 2003; published 2 October 2003)

We performed the systematic optical and transport experiment for $\text{La}_{2-x}\text{Sr}_x\text{CuO}_4$ at high temperatures. The in-plane resistivity $\rho_{ab}(T)$ saturates not at the classical Ioffe-Regel-Mott limit but at much higher value. The in-plane optical conductivity $\sigma_{ab}(\omega)$ exhibits at high temperatures a less characteristic, nearly flat spectrum over a wide energy range up to 1 eV without a Drude peak, irrespective of the positive slope of ρ_{ab} . For small ω , $\sigma_{ab}(\omega)$ even possesses a broad finite-energy peak at high temperatures, suggesting “dynamical” localization. These characteristics are explained in terms of the breakdown of the quasiparticle picture due to strong scattering.

DOI: 10.1103/PhysRevB.68.134501

PACS number(s): 74.72.Dn, 72.15.Lh, 78.20.-e

The problem of resistivity saturation,^{1,2} which was first argued in 1970's, has been revisited recently,³ because resistivity of a wide range of strongly correlated metals does not saturate at the Ioffe-Regel-Mott (IRM) criterion ρ_{IRM} and can increase to a far higher value than ρ_{IRM} . Although the recent theoretical studies⁴⁻⁶ show that absence of resistivity saturation is not necessarily more mysterious than appearance of the saturation, these studies simultaneously reveal that neither behavior is well understood yet. The conventional scheme of the charge transport, the semiclassical Boltzmann theory, should be updated. The problem of high-temperature charge transport is essentially related to breakdown of the quasiparticle picture, which is the basis of the Boltzmann theory. For overall understanding, complex dielectric function $\hat{\epsilon}(\omega)$ or optical conductivity $\sigma(\omega) = (\omega/4\pi)\text{Im}\hat{\epsilon}(\omega)$ is indispensable besides the dc value.

We made systematic measurements of in-plane reflectivity R_{ab} and resistivity ρ_{ab} at high temperatures for $\text{La}_{2-x}\text{Sr}_x\text{CuO}_4$ (LSCO) over a wide x range 0.03–0.25. Although LSCO does not exhibit resistivity saturation at ρ_{IRM} , it shows the saturation at much higher resistivity, which is in proportion to $1/x$. At high temperatures, $\sigma_{ab}(\omega)$ exhibits a less characteristic feature up to 1 eV; a metallic Drude peak centered at $\omega=0$ disappears and instead a broad finite-energy peak dominates the charge dynamics. The charge carriers are “dynamically” localized at high temperatures.

Single crystals of LSCO were grown by a traveling-solvent-floating-zone method.⁷ The superconducting transition temperatures T_c determined by dc resistivity are 12 K ($x=0.06$), 24 K (0.08), 30 K (0.10), 41 K (0.15), and 17 K (0.25). Temperature (T) dependence of the in-plane resistivity ρ_{ab} was measured at 4.2–1000 K using a four-probe method. Resistivity above 300 K was measured in air for $x \leq 0.10$ or under flowing O_2 gas for $x \geq 0.06$. There is negligibly small difference between the $\rho_{ab}(300\text{ K})$ values measured before and after heating up to 1000 K. For $x = 0.06$ –0.10, both ρ_{ab} data measured under different atmosphere were identical. In addition, for representative compositions we also measured ρ_{ab} below 300 K on the sample quenched from 1000 K to liquid N_2 after annealing for 20 hours under the same atmosphere for the high- T resistivity

measurement, but no difference was observed. These results ensure that the oxygen content was not changed during the high- T resistivity measurement. For each composition, we measured ρ_{ab} of several crystals in order to verify that the scattering of the data was within the dimensional error ($\pm 4\%$).

Near-normal incident in-plane ($E \perp c$) reflectivity spectra $R_{ab}(\omega)$ were measured using a Fourier-type interferometer (0.004–1.6 eV) and a grating spectrometer (0.8–6.6 eV). As a reference mirror, we used an evaporated Au film for the far-to-near-infrared (near-IR) regions and Ag film for the visible region. The experimental error of reflectivity ΔR determined by the reproducibility was less than 1% for the far-IR to visible regions and less than 2% for the ultraviolet region. We deduce optical conductivity $\sigma_{ab}(\omega)$ from $R_{ab}(\omega)$ via a Kramers-Kronig transformation. For the extrapolation in the low energy, we assumed a Hagen-Rubens (HR) formula. The parameters in the HR extrapolations, $\sigma_{ab}(0)$, are roughly identical to the measured σ_{dc} values (Fig. 1). Although differences in the extrapolation procedures have a minor effect on the absolute value of σ_{ab} at 4–8 meV, the qualitative behavior (ω dependence) of σ_{ab} is not affected. Above 8 meV, σ_{ab} is independent of extrapolation. We measured R_{ab} at each temperature up to 6.6 eV, and above 6.6 eV we assumed room-temperature data in Ref. 8. Such a procedure is reasonable because R_{ab} exhibits negligible variation with respect to T at 3–6.6 eV. The reflectivity spectra are not shown here, but they are shown in our previous report⁹ for $x = 0.08$.

Figure 1 shows $\rho_{ab}(T)$ for LSCO. At the low temperatures, ρ_{ab} gradually changes from insulating ($d\rho/dT < 0$) to metallic ($d\rho/dT > 0$) behavior, with increasing x , and shows the superconducting transition for $x = 0.06$ –0.25. At the moderate and high temperatures, ρ_{ab} exhibits the metallic character for *all* x . However, we observe a decrease in the slope of ρ_{ab} at high temperatures. Although this feature becomes less pronounced upon Sr doping, it is still noticeable even for $x = 0.10$. A correction from the constant-pressure resistivity ρ_p , obtained from experiments, to the constant-volume resistivity ρ_v , used for theoretical considerations, makes the decrease in the slope more obvious;¹⁰ the reduc-

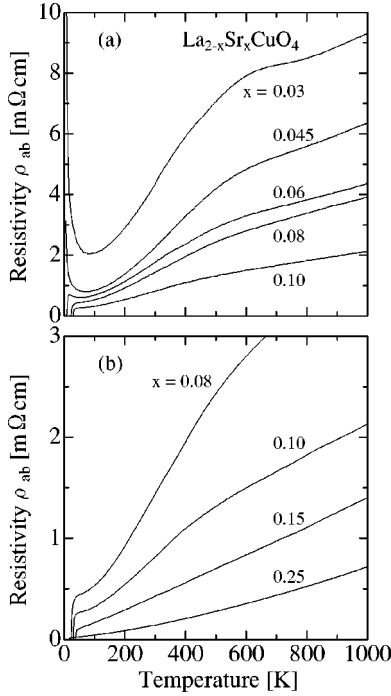


FIG. 1. In-plane resistivity $\rho_{ab}(T)$ of $\text{La}_{2-x}\text{Sr}_x\text{CuO}_4$ up to 1000 K. (a) $x=0.03-0.10$; (b) $x=0.08-0.25$.

tion of the slope becomes confirmable even for $x=0.25$ after the correction (Fig. 2). We may call this reduction of the slope *resistivity saturation*. Saturation does not necessarily mean that the resistivity becomes T independent.^{1,4}

First, we discuss whether this resistivity saturation can be explained within the classical framework. Before discussing the main subject, we consider the physical meanings of the IRM criterion. Concerning Anderson localization at low temperatures, ρ_{IRM} is defined as the resistivity value at $l \sim \lambda_F$ (l , mean free path; λ_F , Fermi wavelength). Around this value, the Boltzmann transport picture breaks down and the concept of mean free path loses its physical meaning. Concerning resistivity saturation at high temperatures, on the other hand, there is another definition of ρ_{IRM} , that is, the resistivity value at $l \sim a$ (a , interatomic spacing). The latter definition is *unrelated* to the breakdown of the Boltzmann picture, but

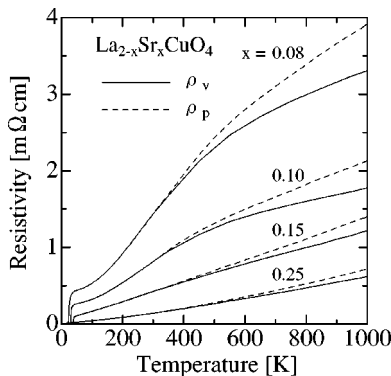


FIG. 2. In-plane resistivity of $\text{La}_{2-x}\text{Sr}_x\text{CuO}_4$ at constant volume (ρ_v , solid line) and at constant pressure ($\rho_p = \rho_{ab}$ in Fig. 1, dashed line).

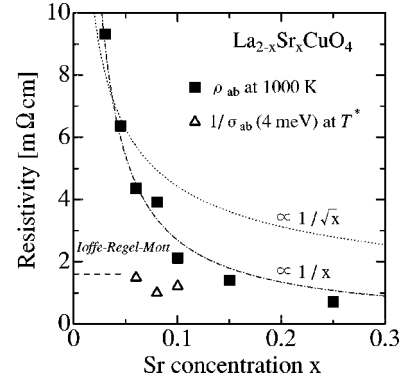


FIG. 3. In-plane resistivity value at 1000 K (solid square) vs Sr concentration x . Correction from ρ_p to ρ_v does not affect the $1/x$ relation. Open triangle represents the critical resistivity value for disappearance of the Drude peak in $\sigma_{ab}(\omega)$ defined as the inverse of $\sigma_{ab}(4 \text{ meV})$ at crossover temperature T^* (250 K, 295 K, and 500 K for $x=0.06, 0.08$, and 0.10 , respectively). It is comparable to ρ_{IRM} (dashed line).

originates from the more intuitive argument, namely, in terms of a tight-binding approximation the shortest mean free path that we can envisage is the interatomic spacing.² However, λ_F becomes comparable to a when the carrier density n is one per unit cell and, therefore, both quantities are not much different except for extremely small n . In addition, the phenomena of localization and saturation are not sharp and the estimation contains ambiguity. Therefore, these two definitions have not been strictly distinguished.² Here, we define ρ_{IRM} as the resistivity value at $l \sim \lambda_F$ even for the argument on the high- T charge transport, following Emery and Kivelson.¹¹ This definition is more closely and directly related to the breakdown of the quasiparticle picture. Remember, we can estimate the ρ value at $l \sim \lambda_F$ but, by contrast, it is difficult to determine the absolute value of l and hence the ρ value at $l \sim a$. The resistivity upturn triggered by Anderson localization provides the ρ value at $l \sim \lambda_F$. It becomes the universal value for two-dimensional (2D) case, as is described afterward.

In the Boltzmann theory, the 2D resistivity is given as $\rho = (h/e^2)(d/k_F l)$ (k_F , Fermi wave number; d , interplane distance). For LSCO, ρ_{IRM} is estimated to be 1.5–1.7 m Ω cm.^{12,13} In 2D metals, the IRM criterion divided by the interplane distance, ρ_{IRM}/d , is the universal sheet resistance $h/e^2 = 25.8 \text{ K}\Omega/\square$, independent of k_F or n . At high temperatures ρ_{ab} becomes much larger than ρ_{IRM} , especially for the slightly doped region, and hence the Boltzmann picture does not seem valid, though ρ_{ab} possesses the positive slope. The resistivity saturates, but the saturated resistivity ρ_{sat} is larger than ρ_{IRM} in LSCO.

Because the Hall-effect study suggests $n \propto x$,¹⁴ one may think that LSCO is an exceptional case in which n is extremely small (λ_F is much longer than a) and hence the large ρ_{sat} is reconciled with the classical picture of saturation at $l \sim a$.¹² However, the following argument suggests that the explanation within the classical framework is not appropriate. The ρ_{ab} value at 1000 K, which may be regarded as ρ_{sat} , is in proportion to $1/x$ (Fig. 3). On the contrary, the classical

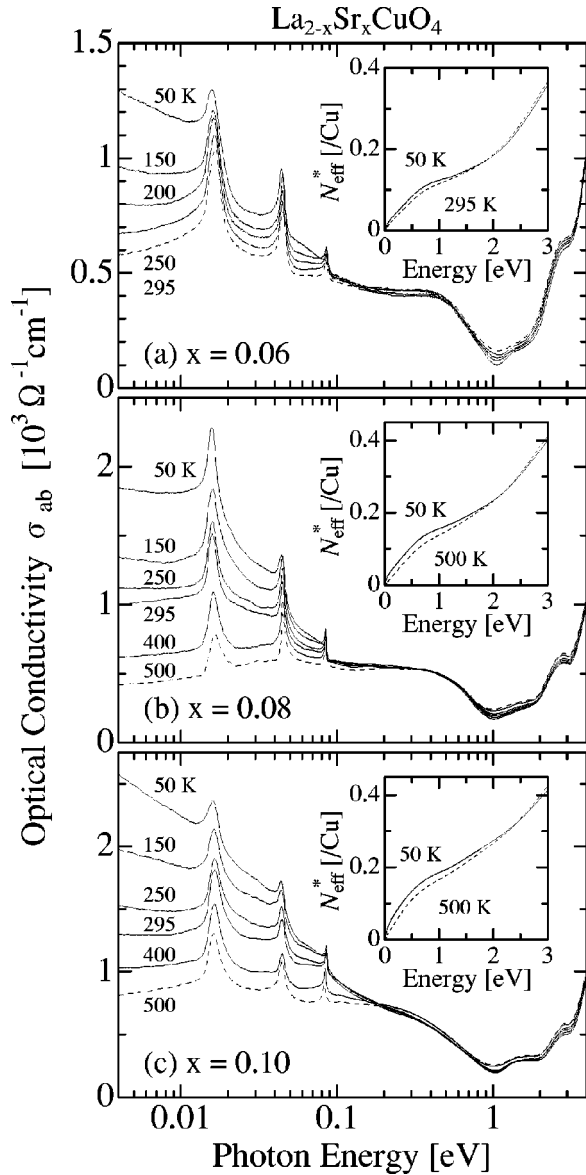


FIG. 4. Temperature-dependent in-plane optical conductivity $\sigma_{ab}(\omega)$ of $\text{La}_{2-x}\text{Sr}_x\text{CuO}_4$ for $x=0.06$ (a), 0.08 (b), and 0.10 (c). Inset shows the integrated spectral weight defined by Eq. (1).

picture predicts that $\rho_{\text{sat}} \propto 1/x^{1/2}$ because of $k_F \propto x^{1/2}$ in the 2D case. Although the correction from ρ_p to ρ_v produces a difference of at the most 15% in the estimate of ρ_{sat} , it does not affect the $1/x$ relation. The enhancement of ρ_{sat} and the relation $\rho_{\text{sat}} \propto 1/x$ seem to be more reasonably ascribed to the correlation effect and/or the characteristic scattering mechanism in LSCO. Calandra and Gunnarsson¹⁵ argue that ρ_{sat} can be enhanced by a factor of $1/x(1-x)$ (or $1/x$ for small x) due to reduction of the kinetic energy by strong correlation effect. The kinetic energy involves a hole hopping to a neighboring site and back. The correlation effect enables this process only when the neighboring site has no hole. Therefore, its probability is in proportion to the product of x (hole occupancy) by $1-x$ (hole empty).

The more direct and convincing evidence supporting the breakdown of the classical picture is obtained from the opti-

cal conductivity (Fig. 4). Three sharp peaks in far-IR region are ascribed to optical phonons¹⁶ and the contribution from the charge carriers is a remaining part below 1 eV. At high temperatures, a Drude peak centered at $\omega=0$ disappears and instead a broad peak centered at 10–30 meV characterizes the low energy $\sigma_{ab}(\omega)$, even for the metallic ($d\rho/dT > 0$) compounds; σ_{ab} even *increases* as a function of ω in the far-IR limit. The spectral weight at the low energies decreases with increasing T and the missing spectral weight is transferred to the higher-energy region. Effective carrier density defined as

$$N_{\text{eff}}^*(\omega) = \frac{2m_0V}{\pi e^2} \int_0^\omega \sigma(\omega') d\omega' \quad (1)$$

(m_0 , bare-electron mass; V , unit-cell volume) suggests that the f -sum rule is fulfilled finally at 2–3 eV (insets of Fig. 4). Consequently, $\sigma_{ab}(\omega)$ becomes less characteristic up to 1 eV at high temperatures. These features are hardly described by l in the classical picture. In that picture, a Drude peak $\sigma(\omega) = \sigma_{\text{dc}}/(\omega^2\tau^2 + 1)$ ($\tau = l/v_F$, relaxation time; v_F , Fermi velocity) still peaks at $\omega=0$ and the integrated spectral weight remains the same, no matter how strong the scattering becomes. The energy scale of the peak width (or $1/\tau$) is at most several times of $k_B T$ and the sum rule is fulfilled around that energy.

The less characteristic conductivity spectrum demonstrates the incoherent electronic states in which the quasiparticle picture breaks down.^{5,17–20} The strong correlation obstructs the growth of the coherence and hence the effect of the inelastic scattering becomes so strong that the periodicity itself is no longer well defined even at accessible high temperatures in experiments. Consequently, the spectral weight, which is condensed at $\omega=0$ when the coherence grows, is dispersed over a wide ω region. This is the strong scattering limit opposite to the weak scattering limit in which the scattering mechanisms are treated as small perturbations against a well-defined periodicity. In such an incoherent state, the concept of mean free path is no longer valid and we should turn back to full quantum-mechanical consideration of the electron self-energy $\Sigma(\omega)$, which is interpreted to be inverse of the relaxation time (or life time) in the quasiparticle picture. The proper language is not a short mean free path, but a broad spectral function (large $\text{Im}\Sigma$).⁵ Whether resistivity saturates depends on the scattering mechanism determining $\Sigma(\omega)$, and ρ can saturate at ρ larger than ρ_{IRM} according to circumstances.

Then, we discuss the conduction process in the high- T incoherent region. An important clue is the broad finite-energy peak in $\sigma_{ab}(\omega)$ at high temperatures. This suggests that a certain collective phenomenon barely survives even in such an incoherent state. Generally, a far-IR peak in $\sigma(\omega)$ is an indication of localization. Indeed, the Drude peak in σ_{ab} disappears when ρ_{ab} becomes comparable to ρ_{IRM} (Fig. 3 of Ref. 9). The charge transport gradually changes from low- T metallic to high- T hopping character. The positive slope of $\rho(T)$ does not necessarily mean the coherent motion of the quasiparticles. With increasing x (and decreasing ρ_{ab}), the

characteristic change in ρ_{ab} and σ_{ab} occurs at higher temperature and becomes inaccessible by experiments.

This high- T localization is different from Anderson localization because at high temperatures inelastic scattering is strong. Anderson localization is formation of the standing waves by the quantum interference effect. Inelastic scattering disturbs this interference. At high temperatures, the correlated charge carriers are “dynamically” localized. With increasing temperature, the scattering becomes strong and the collapse of the periodicity becomes violent. Therefore, ρ has the positive slope in spite of localization. Similar behaviors have been reported also for other bad metals.^{21–25} Since this dynamical localization is arising from loss of the periodicity and is independent of the details of the respective scattering mechanism, it is more essential than whether the saturation is observed in measured ρ .

A finite-energy peak in σ_{ab} has been reported from other groups for LSCO and assigned to polaron,²⁶ disorder,²⁷ or the charged stripes.^{28–30} The present argument of dynamical localization is based on the universality of the finite-energy peak, that is, this peak is commonly observed for materials with different electrical and magnetic properties, including materials without the charged stripes and good metals with low resistivity.³¹

Lastly, we refer to the argument related to the charged stripes.³² Ando *et al.*³³ proposed that the microscopic phase separation into the metallic paths (charged stripes) and the

insulating domains (antiferromagnetic regions) may offer an explanation of the apparent small k_{Fl} in the regime where ρ_{ab} has a positive slope. The present optical study shows the limitations of their approach, which is persistently based on the Boltzmann picture. However, the charged-stripe model itself deserves further investigation because it may be a concrete example of the dynamical localization; the thermal vibration in the stripes destroys the metallic path itself as well as scatters the carriers.

In summary, we have verified the high- T incoherent state in which the quasiparticle picture breaks down and discussed the charge transport there based on the systematic resistivity and optical conductivity data of $\text{La}_{2-x}\text{Sr}_x\text{CuO}_4$. In the high- T incoherent region, the charge carriers are dynamically localized, irrespective of the positive slope of the resistivity, due to strong inelastic scattering. The resistivity saturates at high temperatures, but the saturated resistivity is much larger than the classical Ioffe-Regel-Mott limit, enhanced by strong correlation effects.

We are grateful to S. Uchida, H. Takagi, and Y. Ando for their helpful comments. We would also like to thank S. Okuyama and N. Kaji for their help in the experiments. This work was financially supported by a Grant-in-Aid for Scientific Research from the Ministry of Education, Culture, Sports, Science and Technology of Japan and by the DAIKO Foundation.

*Present address: RIKEN (The Institute of Physical and Chemical Research), Wako 351-0198, Japan; Electronic address: k-takenaka@postman.riken.go.jp

¹P.B. Allen, in *Superconductivity in d- and f-Band Metals*, edited by H. Suhl and M.B. Maple (Academic Press, New York, 1980), p. 291.

²N.F. Mott, *Metal-Insulator Transitions*, 2nd ed. (Taylor & Francis, London, 1990).

³P.B. Allen, *Nature (London)* **405**, 1007 (2000); *Physica B* **318**, 24 (2002).

⁴A.J. Millis, J. Hu, and S. Das Sarma, *Phys. Rev. Lett.* **82**, 2354 (1999).

⁵O. Gunnarsson and J.E. Han, *Nature (London)* **405**, 1027 (2000).

⁶M. Calandra and O. Gunnarsson, *Phys. Rev. Lett.* **87**, 266601 (2001).

⁷Y. Nakamura and S. Uchida, *Phys. Rev. B* **47**, 8369 (1993).

⁸S. Uchida, T. Ido, H. Takagi, T. Arima, Y. Tokura, and S. Tajima, *Phys. Rev. B* **43**, 7942 (1991).

⁹K. Takenaka, R. Shiozaki, S. Okuyama, J. Nohara, A. Osuka, Y. Takayanagi, and S. Sugai, *Phys. Rev. B* **65**, 092405 (2002).

¹⁰B. Sundqvist and E.M.C. Nilsson, *Phys. Rev. B* **51**, 6111 (1995).

¹¹V.J. Emery and S.A. Kivelson, *Phys. Rev. Lett.* **74**, 3253 (1995).

¹²H. Takagi, B. Batlogg, H.L. Kao, J. Kwo, R.J. Cava, J.J. Krajewski, and W.F. Peck, Jr., *Phys. Rev. Lett.* **69**, 2975 (1992).

¹³Y. Fukuzumi, K. Mizuhashi, K. Takenaka, and S. Uchida, *Phys. Rev. Lett.* **76**, 684 (1996).

¹⁴H. Takagi, T. Ido, S. Ishibashi, M. Uota, S. Uchida, and Y. Tokura, *Phys. Rev. B* **40**, 2254 (1989).

¹⁵M. Calandra and O. Gunnarsson, *Europhys. Lett.* **61**, 88 (2003).

¹⁶Optical phonons are screened upon carrier doping in some

studies,^{26,29,30} while they remain sharp, like this work, in others [R.T. Collins, Z. Schlesinger, G.V. Chandrashekar, and M.W. Shafer, *Phys. Rev. B* **39**, 2251 (1989); F. Gao, D.B. Romero, D.B. Tanner, J. Talvacchio, and M.G. Forrester, *ibid.* **47**, 1036 (1993); M.A. Quijada, D.B. Tanner, F.C. Chou, D.C. Johnston, and S.-W. Cheong, *ibid.* **52**, 15 485 (1995)]. There is even an argument that poor screening is an important general character of the cuprates [C.C. Homes, A.W. McConnell, B.P. Clayman, D.A. Bonn, Ruixing Liang, W.N. Hardy, M. Inoue, H. Negishi, P. Fournier, and R.L. Greene, *Phys. Rev. Lett.* **84**, 5391 (2000)]. The discrepancy may originate from difference in samples and/or surface condition.

¹⁷M. Imada, A. Fujimori, and Y. Tokura, *Rev. Mod. Phys.* **70**, 1039 (1998).

¹⁸O. Parcollet and A. Georges, *Phys. Rev. B* **59**, 5341 (1999).

¹⁹J. Jaklič and P. Prelovšek, *Adv. Phys.* **49**, 1 (2000).

²⁰J. Merino and R.H. McKenzie, *Phys. Rev. B* **61**, 7996 (2000).

²¹A.A. Tsvetkov, J. Schützmann, J.I. Gorina, G.A. Kaljushnaia, and D. van der Marel, *Phys. Rev. B* **55**, 14 152 (1997).

²²P. Kostic, Y. Okada, N.C. Collins, Z. Schlesinger, J.W. Reiner, L. Klein, A. Kapitulnik, T.H. Geballe, and M.R. Beasley, *Phys. Rev. Lett.* **81**, 2498 (1998).

²³K. Takenaka, R. Shiozaki, and S. Sugai, *Phys. Rev. B* **65**, 184436 (2002).

²⁴Y.S. Lee, Jaejun Yu, J.S. Lee, T.W. Noh, T.-H. Gimm, Han-Yong Choi, and C.B. Eom, *Phys. Rev. B* **66**, 041104 (2002).

²⁵N.L. Wang, P. Zheng, T. Feng, G.D. Gu, C.C. Homes, J.M. Tranquada, B.D. Gaulin, and T. Timusk, *Phys. Rev. B* **67**, 134526 (2003).

- ²⁶R.P.S.M. Lobo, F. Gervais, and S.B. Oseroff, *Europhys. Lett.* **37**, 341 (1997).
- ²⁷T. Startseva, T. Timusk, M. Okuya, T. Kimura, and K. Kishio, *Physica C* **321**, 135 (1999).
- ²⁸M. Dumm, D.N. Basov, S. Komiya, Y. Abe, and Y. Ando, *Phys. Rev. Lett.* **88**, 147003 (2002).
- ²⁹F. Venturini, Q.-M. Zhang, R. Hackl, A. Lucarelli, S. Lupi, M. Ortolani, P. Calvani, N. Kikugawa, and T. Fujita, *Phys. Rev. B* **66**, 060502 (2002).
- ³⁰A. Lucarelli, S. Lupi, M. Ortolani, P. Calvani, P. Maselli, M. Capizzi, P. Giura, H. Eisaki, N. Kikugawa, T. Fujita, M. Fujita, and K. Yamada, *Phys. Rev. Lett.* **90**, 037002 (2003).
- ³¹We do not discuss the finite-energy peak at *low* temperatures, which is reported by some of other studies. An important point of the present result is that the finite-energy peak appears at *high* temperatures even though ρ is metallic and a Drude peak appears at low temperatures.
- ³²S.A. Kivelson, E. Fradkin, and V.J. Emery, *Nature (London)* **393**, 550 (1998).
- ³³Y. Ando, A.N. Lavrov, S. Komiya, K. Segawa, and X.F. Sun, *Phys. Rev. Lett.* **87**, 017001 (2001).